*Article*

# A Theoretical and Experimental Study for Enzymatic Biodiesel Production from Babassu Oil (*Orbignya* sp.) Using Eversa Lipase

Jeferson Yves Nunes Holanda Alexandre [1], Francisco Thálysson Tavares Cavalcante [1], Lara Matias Freitas [2], Alyne Prudêncio Castro [3], Pedro Tavares Borges [4], Paulo Gonçalves de Sousa Junior [5], Manoel Nazareno Ribeiro Filho [4], Ada Amelia Sanders Lopes [4], Aluisio Marques da Fonseca [6], Diego Lomonaco [5], Maria Alexsandra de Sousa Rios [3] and José Cleiton Sousa dos Santos [1,4,*]

[1] Departamento de Engenharia Química, Campus do Pici, Universidade Federal do Ceará, Fortaleza 60455760, CE, Brazil

[2] Programa de Pós Graduação em Ciências Naturais, Universidade Estadual do Ceará, Fortaleza 60714903, CE, Brazil

[3] Departamento de Engenharia Mecânica e de Produção da UFC, Universidade Federal do Ceará-Bloco 714-Campus do Pici, Fortaleza 60455-900, CE, Brazil

[4] Instituto de Engenharias e Desenvolvimento Sustentável, Universidade da Integração Internacional da Lusofonia Afro-Brasileira, Campus das Auroras, Redenção 62790970, CE, Brazil

[5] Department of Organic and Inorganic Chemistry, Federal University of Ceara, Fortaleza 60440-900, CE, Brazil

[6] Mestrado Acadêmico em Sociobiodiversidades e Tecnologias Sustentáveis—MASTS, Instituto de Engenharias e Desenvolvimento Sustentável, Universidade da Integração Internacional da Lusofonia Afro-Brasileira, Acarape 62785-000, CE, Brazil

* Correspondence: jcs@unilab.edu.br

**Abstract:** A theoretical and experimental study was carried out on the biocatalytic production of babassu biodiesel through enzymatic hydroesterification. The complete hydrolysis of babassu oil was carried out using a 1:1 mass solution at 40 °C for 4 h using 0.4% of lipase from *Thermomyces lanuginosus* (TLL). Then, with the use of Eversa® Transform 2.0 lipase in the esterification step, a statistical design was used, varying the temperature (25–55 °C), the molar ratio between free fatty acids (FFAs) and methanol (1:1 to 1:9), the percentage of biocatalyst (0.1% to 0.9%), and the reaction time (1–5 h) using the Taguchi method. The ideal reaction levels obtained after the statistical treatment were 5 h of reaction at 40 °C at a molar ratio of 1:5 (FFAs/methanol) using 0.9% of the biocatalyst. These optimal conditions were validated by chromatographic analysis; following the EN 14103 standard, the sample showed an ester concentration of 95.76%. A theoretical study was carried out to evaluate the stability of Eversa with FFAs. It was observed in the molecular docking results that the ligands interacted directly with the catalytic site. Through molecular dynamics studies, it was verified that there were no significant conformational changes in the studied complexes. Theoretical and experimental results show the feasibility of this process.

**Keywords:** biodiesel; hydroesterification; Taguchi method; molecular docking; molecular dynamics

## 1. Introduction

Petroleum is the most used fossil fuel in the world since, when refined, it generates several by-products such as diesel, gasoline, and lubricants, among others [1]. Because of this, the United States International Energy Agency (IEA) estimates that there will be a global oil supply deficit from 2025 onwards [2]. Thus, renewable fuels emerge as a viable alternative to meet this energy demand [3]. Renewable fuels, also known as biofuels, are materials with energy applications from agricultural products such as sugars, animal and vegetable oils, and forest biomass, among others. Among the fuels from renewable sources,

biodiesel stands out. This material can partially replace diesel in internal combustion engines [4].

Benefits such as excellent lubricity, accessible transport, storage, and lower toxicity and environmental damage make biodiesel an excellent alternative to diesel. Biodiesel can be obtained from vegetable oil, animal fat, and residual oil [3]. Oil sources are formed by condensing fatty acids and glycerol, forming glycerides [5]. It is worth mentioning that the physiological characteristics of the oil source used directly influence the properties of the oil and, consequently, the physicochemical characteristics of the biodiesel produced [6]. Due to the factors mentioned above, this work studied the application of babassu oil (*Attalea speciosa*) in the ecological production of biodiesel. The babassu fruit was chosen because it is present in about 196.000 km$^2$ of the Brazilian territory, with most palm trees located in the northern and northeastern regions [7,8].

As biodiesel is formed mainly by esters, it is necessary to apply chemical processes to transform oils, such as thermal cracking, esterification, and transesterification [9]. However, the synthesis via hydroesterification has been widely studied since this process can be carried out with any oil source, regardless of its purity, acidity, and humidity [10]. Except for thermal cracking, these processes can be performed in the presence of homogeneous, heterogeneous, or enzymatic catalysts. Enzymatic catalysts are a viable alternative among the various types of existing catalysts, as these materials generate less waste and are less harmful to the environment when compared to chemical catalysts [11–15].

However, problems are associated with applying biocatalysts on an industrial scale since these materials have a high price and low operational stability. Thus, several strategies are employed to expand the application of biocatalysts in the industry [16–20]. Techniques of enzymatic immobilization, green solvents, and genetic manipulation in the production of enzymes are some techniques that can be used [21].

Genetic manipulation is used in the production of soluble enzymes, and this modification can increase the activity of the enzyme. In addition, genetically modified enzymes can be commercialized with a value of 30 to 50 times lower than their immobilized alternatives. Eversa® Transform 2.0 stands out among the genetically manipulated enzymes. This biological material is produced through the genetic modification of the lipase of *Thermomyces lanuginosus* expressed in a strain of *Aspergillus oryzae*. This biocatalyst was designed to be an economically viable material that can be applied in reactions to produce free fatty acids, glycerides, and biolubricants [22–24].

Thus, understanding the behavior of Eversa lipase at the molecular level through computational tools and the optimization of the reaction process can facilitate the application of these materials on a large scale. Thus, the present study proves to be an alternative for the development of future babassu biodiesel synthesis processes using Eversa lipase as a biocatalyst. [25]. Thus, the present work sought to evaluate the potential of Eversa® Transform 2.0 lipase in synthesizing babassu methyl esters (FAMEs). For the production of FAMEs, enzymatic hydroesterification was used since this strategy has less impact on the environment when compared to conventional routes [26,27]. In addition, theoretical studies of the esterification stage were carried out. Molecular docking was used to obtain the best conformation between the fatty acids and the enzyme's catalytic site and to understand the nature of these interactions. In molecular dynamics studies, the stability of the enzyme–substrate complex under reactional production conditions was evaluated.

## 2. Results and Discussion

### 2.1. Enzymatic Hydrolysis

The proposed enzymatic hydrolysis was performed satisfactorily since there was an increase in the acidity index of the oil from 0.75 mg NaOH/g to 127.03 mg NaOH/g. The acidity index obtained is consistent with expectations since refined babassu oil was used during hydrolysis. Carvalho et al. (2021) [22] performed the complete hydrolysis of refined and residual soybean oil within 3 h of reaction. In this process, *Candida rugosa*-free lipase was used as a biocatalyst.

## 2.2. Taguchi Planning-Optimization of the Production of Methyl Esters of Babassu Fatty Acids

In this stage of the work, Taguchi planning with an orthogonal matrix L9 was used. This strategy was employed to optimize and reduce the number of trials. Furthermore, this method makes it possible to understand the effects and interaction of parameters related to the process [28–30]. Table 1 shows the results obtained relating them to the proposed reaction parameters. It is worth noting that all experiments were performed in triplicate and that the results remained within the expected margin of error.

**Table 1.** Experimental Taguchi design for the production of methyl esters from babassu.

| Reaction | Time (h) | Temperature (°C) | Molar Ratio (FFA/Methanol) | Biocatalyst (% w/w) | Conversion (%) | S/N |
|---|---|---|---|---|---|---|
| 1 | 1 | 25 | 1:1 | 0.1 | 3.16 ± 0.48 | 9.99 |
| 2 | 1 | 40 | 1:5 | 0.5 | 58.79 ± 0.078 | 35.39 |
| 3 | 1 | 55 | 1:9 | 0.9 | 19.43 ± 0.66 | 25.77 |
| 4 | 3 | 25 | 1:5 | 0.9 | 95.20 ± 0.031 | 39.57 |
| 5 | 3 | 40 | 1:9 | 0.1 | 7.75 ± 0.30 | 17.79 |
| 6 | 3 | 55 | 1:1 | 0.5 | 8.44 ± 0.53 | 18.52 |
| 7 | 5 | 25 | 1:9 | 0.5 | 94.65 ± 0.036 | 39.52 |
| 8 | 5 | 40 | 1:1 | 0.9 | 75.36 ± 0.51 | 37.54 |
| 9 | 5 | 55 | 1:5 | 0.1 | 2.80 ± 0.18 | 8.94 |

Based on the data in Table 1, it was possible to observe that test 4 presented the best conversion and signal-to-noise ratio (S/N) results, 95.20 ± 0.031 and 39.57, respectively. In this assay, 0.9% of biocatalyst was used, with a molar ratio of 1:5 (FFA/methanol), for 3 h of reaction at 40 °C. It was observed that the percentage of biocatalysts significantly influenced the process since the experiments using 0.9% of catalyst (experiments 3, 4, and 8) presented, on average, better results in conversion and signal-to-noise ratio when compared to tests conducted with 0.1 and 0.5% of the biocatalyst. In order to identify the influence of temperature, time, and molar ratio, further statistical analysis is necessary.

### 2.2.1. S/N Ratio Analysis

Taguchi planning employs S/N relationships to identify the impact of parameters on the process. In this work, the "bigger is better" function was used to determine the S/N ratios since the present planning was intended to obtain a higher conversion. Table 2 shows the S/N averages for the individual factors and levels. Furthermore, the table shows the delta values. These values were calculated through the difference between each factor's highest and lowest S/N ratio. Through the delta values, it is possible to assess the impact of the levels on the process and therefore identify the parameters that had the most significant influence.

**Table 2.** Response to the averages of the S/N ratios.

| Factors/Levels | Time (h) | Temperature (°C) | The Molar Ratio (FFA/Methanol) | Biocatalyst (% w/w) |
|---|---|---|---|---|
| 1 | 23.72 | 29.70 | 22.02 | 12.24 |
| 2 | 25.29 | 30.24 | 27.97 | 31.14 |
| 3 | 28.67 | 17.74 | 27.69 | 34.29 |
| Delta | 4.95 | 12.50 | 5.95 | 22.05 |
| Ranking | 4 | 2 | 3 | 1 |

It is possible to observe that the amount of biocatalyst and temperature were the most influential variables in the process, as they presented the highest delta values, 22.05 and 12.50, respectively. Thus, the data in Table 2 confirm the influence of the percentage of biocatalysts and the temperature on the process. It is evident that the increase in the

percentage of biocatalysts in the reaction medium from level 1 (0.1%) to level 3 (0.9%) significantly increased the response of the S/N ratio and, consequently, the conversion. This expansion can be attributed to the increased catalytic sites in the reaction medium. This availability is related to a more significant number of reactions coinciding [31].

On the other hand, the temperature showed different behavior. It was observed that the change from level 1 (25 °C) to level 2 (40 °C) favored the expansion of the conversion. However, the change from level 2 (40° C) to level 3 (55 °C) had the opposite effect. This is because enzymes are sensitive biological materials that operate in a specific temperature range. In addition, an excessive temperature increase can reduce activity, leading to deactivation [32]. Finally, the molar ratio and reaction time factors proved less effective in the process, with delta values equal to 6.75 and 3.73, respectively. It was observed that the amplification of methanol in the reaction medium from level 1 (1:1 FFA/methanol) to level 2 (1:5 1 FFA/methanol) significantly impacted the response of the S/N ratio and, consequently, the conversion. However, switching from level 2 (1:5 1 FFA/methanol) to level 3 (1:9 1 FFA/methanol) showed a slight drop in response. This low variance can be attributed to Eversa's high resistance to methanol since this enzyme was developed to produce methyl ester [33]. The low variation in the response of the S/N ratio over time may be associated with high enzyme activity so that, according to the data shown in Table 1, it is possible to obtain 95.20 ± 0.029 (assay 4) in 3 h of reaction.

### 2.2.2. Analysis of Variance (ANOVA)

Conversion data obtained through experimental design were statistically evaluated using Analysis of Variance (ANOVA). According to the literature, the *p*-value ensures the significance of each factor for the process studied. Table 3 shows the results obtained in the ANOVA.

**Table 3.** Analysis of variance of the parameters that affect the esterification of babassu oil.

| Factors | SS | DF | MS | *F*-value | *p*-Value | Contribution (%) |
|---------|-----|-----|--------|-----------|-----------|------------------|
| Time | 38.40 | 2 | - | - | - | 3.05% |
| Temperature | 299.30 | 2 | 149.65 | 7.79 | 0.11 | 23.77% |
| Molar ratio | 67.62 | 2 | 33.812 | 1.76 | 0.36 | 5.37% |
| Biocatalyst | 853.63 | 2 | 426.817 | 22.23 | 0.043 | 67.80% |
| Residual | 38.40 | 2 | 19.20 | | | - |
| Total | 1258.98 | 6 | - | - | - | |

In order to ensure the significance of a factor with a 95% confidence interval, the p-value must be less than 0.05. Thus, the table clarifies that among the factors studied, only the percentage of biocatalysts showed significance with a *p*-value equal to 0.043 and a contribution percentage equal to 67.80%. Moreira et al. (2020) [26] studied the production of ethyl esters from babassu. The researchers reported that the percentage of biocatalysts was the most influential parameter in the process, with a *p*-value equal to that obtained in this work. Sun, Guo, and Chen (2021) [34] studied the production of ethyl biodiesel from Semen Abutili *(Abutilon theophrasti Medic.)*, using Eversa® Transform 2.0 in its liquid form as a catalyst. During the study, the authors verified the influence of the biocatalyst on the reaction rate, and it was observed that the increase in the percentage of biocatalysts from 1% to 6% increased the production rate of esters in the same proportion. Thus, the results obtained in this work are in agreement with the literature data since, as mentioned above, the increase in the percentage of the biocatalyst is related to the increase in the availability of active sites and, consequently, to the more significant number of reactions coinciding [32]. It is worth noting that this work demonstrated that babassu oil could be a viable alternative for producing FAME, as a smaller amount of biocatalyst was used in a shorter time when compared to authors such as Sun, Guo, and Chen (2021) [34].

After statistical analysis and discussion of the collected data, the optimal conditions for the production of methyl esters were defined based on the range of levels (1, 2, and 3) of

each factor (time, temperature, molar ratio (FFA/methanol) and percentage of biocatalyst), i.e., time (5 h), temperature (40 °C), the molar ratio (1:5 FFA/methanol), and percentage of biocatalyst (0.9% *w/w*). Under these conditions, the theoretical conversion was 98.64%. These optimal conditions were validated by the chromatographic analysis of methyl esters, following the EN 14103 standard with some modifications. The sample showed an ester concentration of 95.76%. This variation of approximately 2.88% is within the expected margin of error, as biocatalysts can quickly lose their catalytic activity as they are more sensitive to external factors than chemical catalysts [35].

### 2.3. Physicochemical Characterization of the Oil Produced

The babassu methyl esters were separated from the by-products (water, glycerin, and alcohol in excess) and characterized regarding their physicochemical properties. The biodiesel produced is within the quality standards established by the "American Society for Testing and Materials" (ASTM), following the specifications of ASTM D6751. According to the standard, the kinematic viscosity at 40 °C of the monoalkyl esters from vegetable oil must be between 1.9 and 6.0 cSt. The produced oil had a viscosity equal to 2.52 cSt. Kinematic viscosity is a property of fluids that relates to a fluid's molecular diffusion momentum. This property is of paramount importance, as it can directly interfere with the motor's efficiency [36]. In addition, the standard establishes that the density at 20 °C is between 860 and 900 Kg/m$^3$, and the density of biodiesel produced from babassu was 872.90 Kg/m$^3$. The specific mass is an intensive property of matter calculated through the ratio between two extensive properties (mass/volume) [37]. Therefore, the results obtained indicate that the biodiesel produced has potential application.

### 2.4. Theoretical Study

#### 2.4.1. Protein Modeling by Homology

The Ramachandran graph was used to validate the homology modeling (Figure 1). This diagram represents all possible combinations of dihedral angles (Ψ versus φ) in the amino acids of a polypeptide chain [38]. This technique exposes the combinations of the excellent stability of these angles, making it possible to validate the probable structure of the biomolecule [39]. According to the diagram, 91.5% of the residues of the modeled protein are in favorable regions (red region), 6.5% of the residues are in the additionally allowed region (Regions a, b, l, p, yellow), 1.6% are located in the generously allowed regions (Regions ~a, ~b, ~l, ~p, i.e., light yellow), and 0.4% are in unfavorable regions (black region). It is worth noting that the residues found in unfavorable regions refer to the structures used as a template. In addition, some residues are located at the ends of the protein [39]. The VERIFY 3D (Figure 2) was used to stipulate the compatibility of an atomic model (3D) with an amino acid sequence (1D) for the modeled protein. The % of residues with a mean 3D-1D score $\geq$ 0.2 are acceptable [25]. In the present study, about 93.71% of the residues had a mean 3D-1D score $\geq$ 0.2. These results show that the proposed model was compatible with its frequency. Thus, the Ramachandran diagram made it possible to identify the regions that maintained the conserved structure and the variable locations with alignment since 91.5% of the modeled protein residues are in favorable regions. Furthermore, VERIFY 3D proved the compatibility of the atomic model (3D) with the amino acid sequence (1D) since the model developed had an average score 3D-1D $\geq$ 0.2 of 93.71%. Therefore, the data from the Ramachandran chart and Verify 3D validate the model obtained in this work.

#### 2.4.2. Molecular Docking

From molecular docking, nine conformations were generated for each ligand and their respective values of binding affinity and mean square deviation of atomic positions (*RMSD*). The best conformation established by *Autodock Vina* was the one that exhibited the lowest values of energy affinity and *RMSD*. Table 4 elucidates the values obtained in the molecular docking of the six substrates studied.
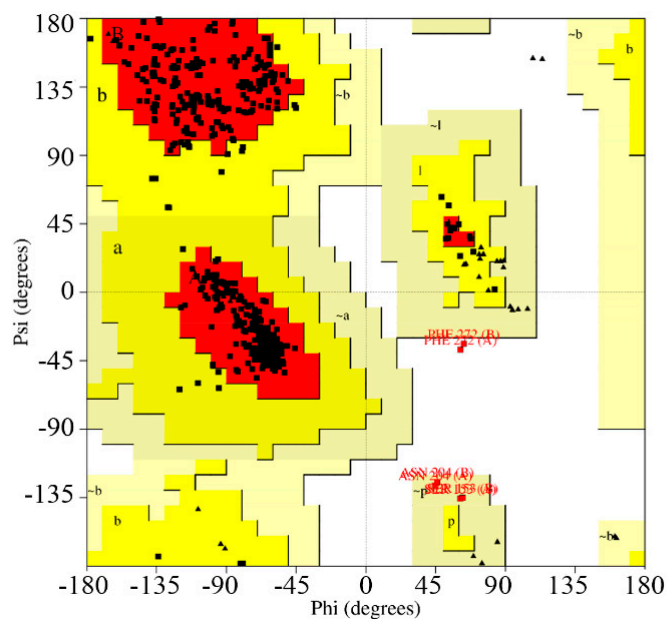
**Figure 1.** Ramachandran plot of protein obtained by homology. (□) Non-glycine and non-proline residues; (Δ) Number of glycine residues.
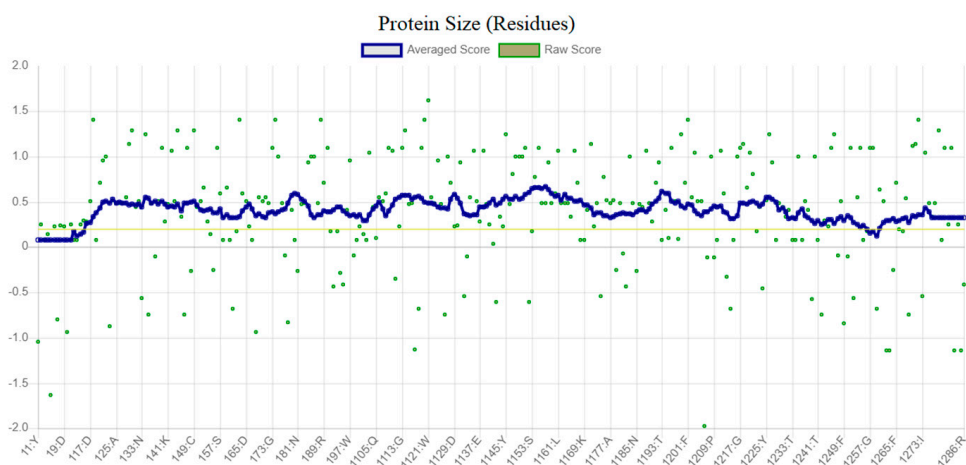


**Figure 2.** Results of structural verification of Eversa® lipase by Verify 3D.

**Table 4.** Results obtained in the molecular docking process.

| Substrate | Chosen Pose | Binding Affinity (kCal/mol) | Vina *RMSD* (Å) |
|---|---|---|---|
| Octanoic acid | 2 | −5.1 | 1.566 |
| Decanoic acid | 2 | −5.4 | 1.561 |
| Dodecanoic acid | 4 | −5.6 | 1.658 |
| Tetradecanoic acid | 2 | −5.8 | 0.970 |
| Hexadecanoic acid | 4 | −5.8 | 2.296 |
| *cis*-9-octadecenoic acid | 5 | −6.2 | 1.426 |

Overall, the ligands showed good binding affinity with the catalytic site. Among the ligands evaluated, oleic acid showed the highest binding affinity. This result suggests that the combination of this substrate with the enzyme was the most stable and suitable for esterification [40]. Furthermore, it is possible to observe a direct relationship between the increase in binding affinity and the increase in the carbonic chain of the esters. This expansion may be related to increased interactions between the ligands and the enzyme's catalytic site [25]. The types of residues involved in the interactions between free fatty acids and Eversa® Transform 2.0 are shown in Table 5 and Figure 3.
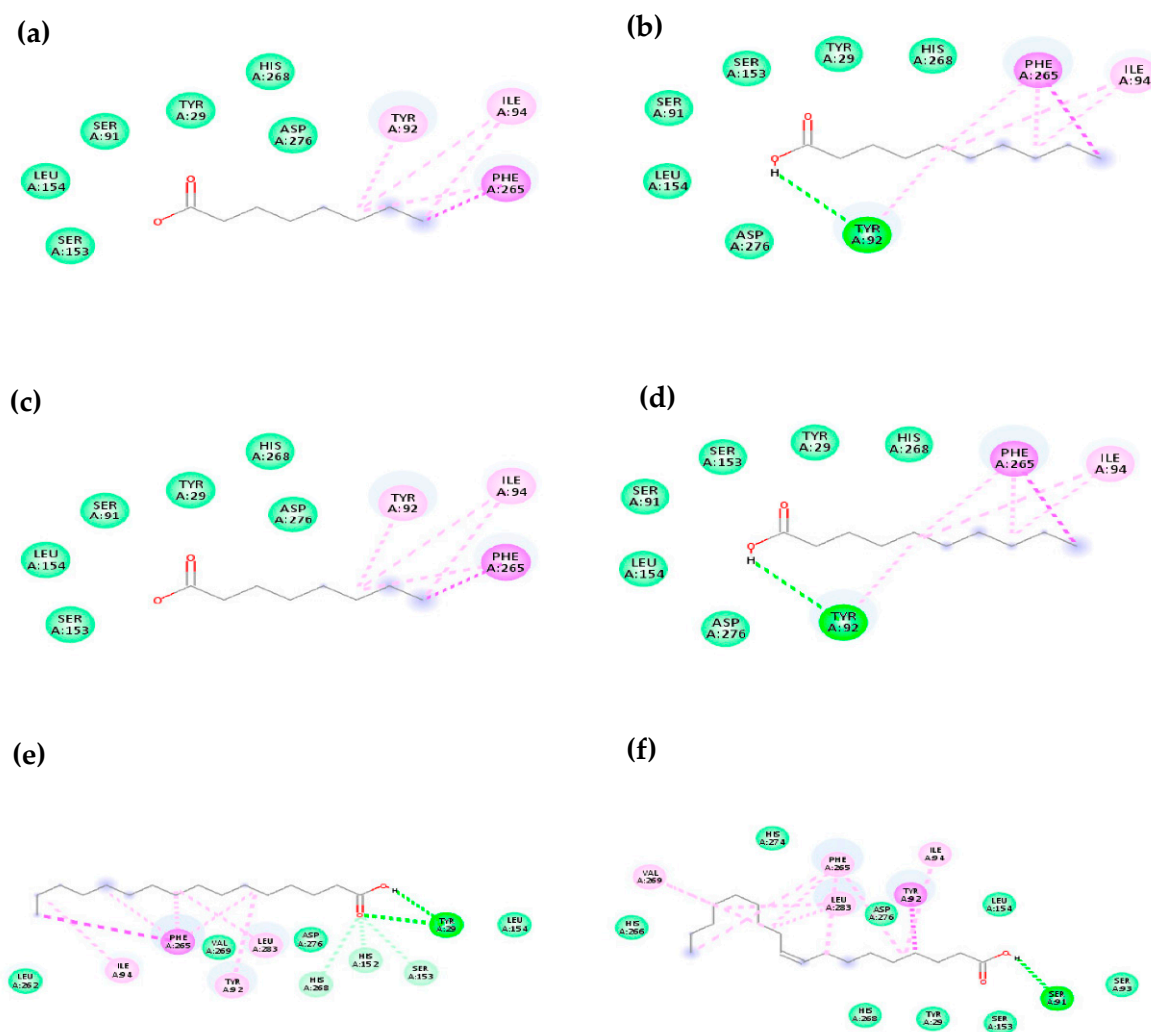


**Figure 3.** Diagrammatic representation of the interactions between the ligands and the enzyme's active site. (**a**) Octanoic acid; (**b**) Decanoic acid; (**c**) Dodecanoic acid; (**d**) Tetradecanoic acid; (**e**) Hexadecanoic acid; (**f**) cis-9-octadecanoic acid.

**Table 5.** Interactions of ligands with lipase after docking.

| Substrate | Waste Involved | | |
|---|---|---|---|
| | Hydrogen Bonds | Van der Waals Interactions | Hydrophobic Interactions |
| Octanoic acid | - | ASP276, HIS268, LEU154, SER91, SER153, TYR29 | ILE94, PHE265, TYR92, |

**Table 5.** *Cont.*

| Substrate | Waste Involved | | |
|---|---|---|---|
| | **Hydrogen Bonds** | **Van der Waals Interactions** | **Hydrophobic Interactions** |
| Decanoic acid | TYR92 (2.94 Å) | ASP276, HIS268 LEU154, SER91, SER153, TYR29 | ILE94, PHE265 |
| Dodecanoic acid | HIS152 (3.06 Å) | ASP276, HIS268, LEU154, SER153, TYR29 | ILE94, LEU262, PHE265, TYR92 |
| Tetradecanoic acid | - | ASP276, HIS266, HIS268, HIS274, ILE94, LEU154, LEU285, SER153, TYR29 | LEU283, PHE265, TYR92, VAL269 |
| Hexadecanoic acid | HIS152 (2.73 Å), HIS268 (2.96 Å), SER153 (2.86 Å), TYR29 (2.78 Å), TYR29 (2.59 Å) | ASP276, LEU154, LEU262, VAL269 | ILE94, LEU283, PHE265, TYR92 |
| *cis*-9-octadecenoic acid | SER 91 (2.27 Å) | APS276, HIS266, HIS268, HIS274, LEU154, TYR29, SER 153, SER93 | ILE94, LEU283, PHE265, VAL269, TYR92 |

The catalytic triad of lipase Eversa® Transform 2.0 comprises ASP206, HIS268, and SER153 [41]. Thus, it is possible to observe that the ligands interacted directly with residues HIS268 and SER153 [42]. In addition, the oxyanion cavity of the enzyme can interact with the substrate since the function of residues in this region is to balance the negative charges of the intermediates formed during the reaction. The oxyanion cavity of lipase Eversa® Transform 2.0 comprises LEU154 and SER91 residues [43]. The residue of the oxyanion region LEU154 interacted with all ligands, in the vast majority, from Van der Waals forces. Electrostatic interactions, hydrogen bonds, hydrophobic interactions, and Van der Waals forces are significant as they stabilize the enzyme–substrate complex [44,45].

Thus, ligand VI showed higher binding affinity. In general, Van der Waals interactions have low binding energy. However, the combination of several Van der Waals forces confers a stabilizing force on the protein–protein and protein–ligand complexes [46]. Most of the time, the first interactions between the enzyme and the substrate are non-covalent. They are electrostatic, Van der Waals, and hydrophobic interactions. Thus, the formation of these interactions may favor the occurrence of a reaction [25,40,47].

2.4.3. Molecular Dynamics Simulations
Root Mean Square Deviation—*RMSD*

It was observed that the ligands studied were correctly accommodated in the catalytic site of lipase Eversa® [48]. Thus, through the lipase–ligand complexes (I–VI), simulation studies were carried out to evaluate not only the conformational changes of the enzyme but also its stability after each conformational change. The Root Mean Square Deviation (*RSMD*) of the lipase–ligand complexes was used to evaluate the extent to which conformational changes occurred in the studied molecule during the simulation time. Figure 4 shows the *RSMD* behaviors of the complexes studied in the equilibration stage.
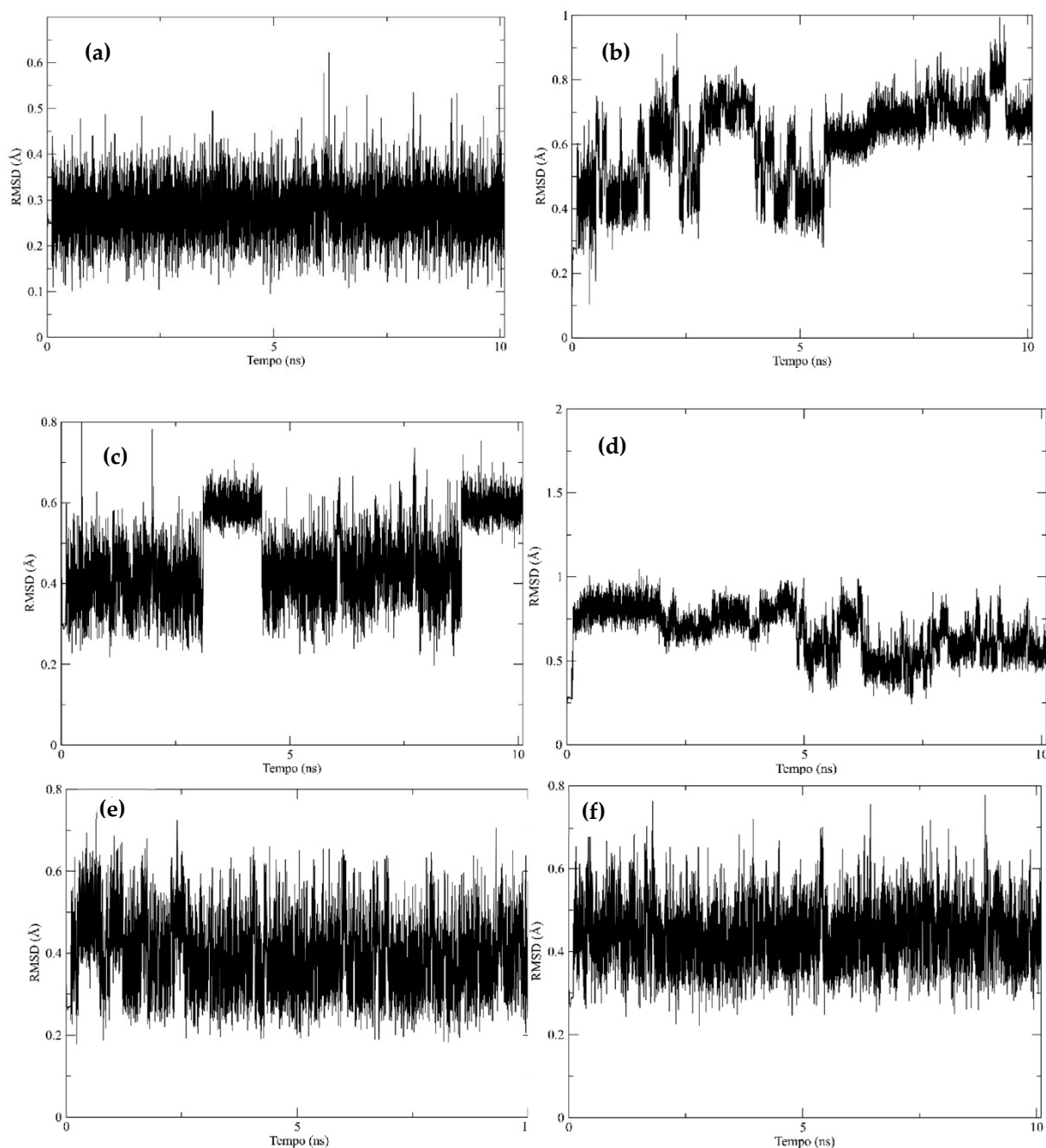
**Figure 4.** Root Mean Square Deviation (*RMSD*) for the initial conformation of the complexes versus the simulation time (nanoseconds) in the equilibration step. (**a**) Octanoic acid; (**b**) Decanoic acid; (**c**) Dodecanoic acid; (**d**) Tetradecanoic acid; (**e**) Hexadecanoic acid; (**f**) *cis*-9-octadecenoic acid.

From the equilibrium simulations of the lipase–ligand complexes in the solvent, it was possible to obtain preliminary information on the behavior of the conformations for the dynamics. In this step, it was observed that the *RSMD* stabilization values of the studied ligands oscillated between 0.25 and 1.0 Å in the evaluated time. These low *RSMD* values may be associated with the movement of ions and solvents in the system during the initial conformation of the complexes. Figure 5 shows the results obtained in the production stage.
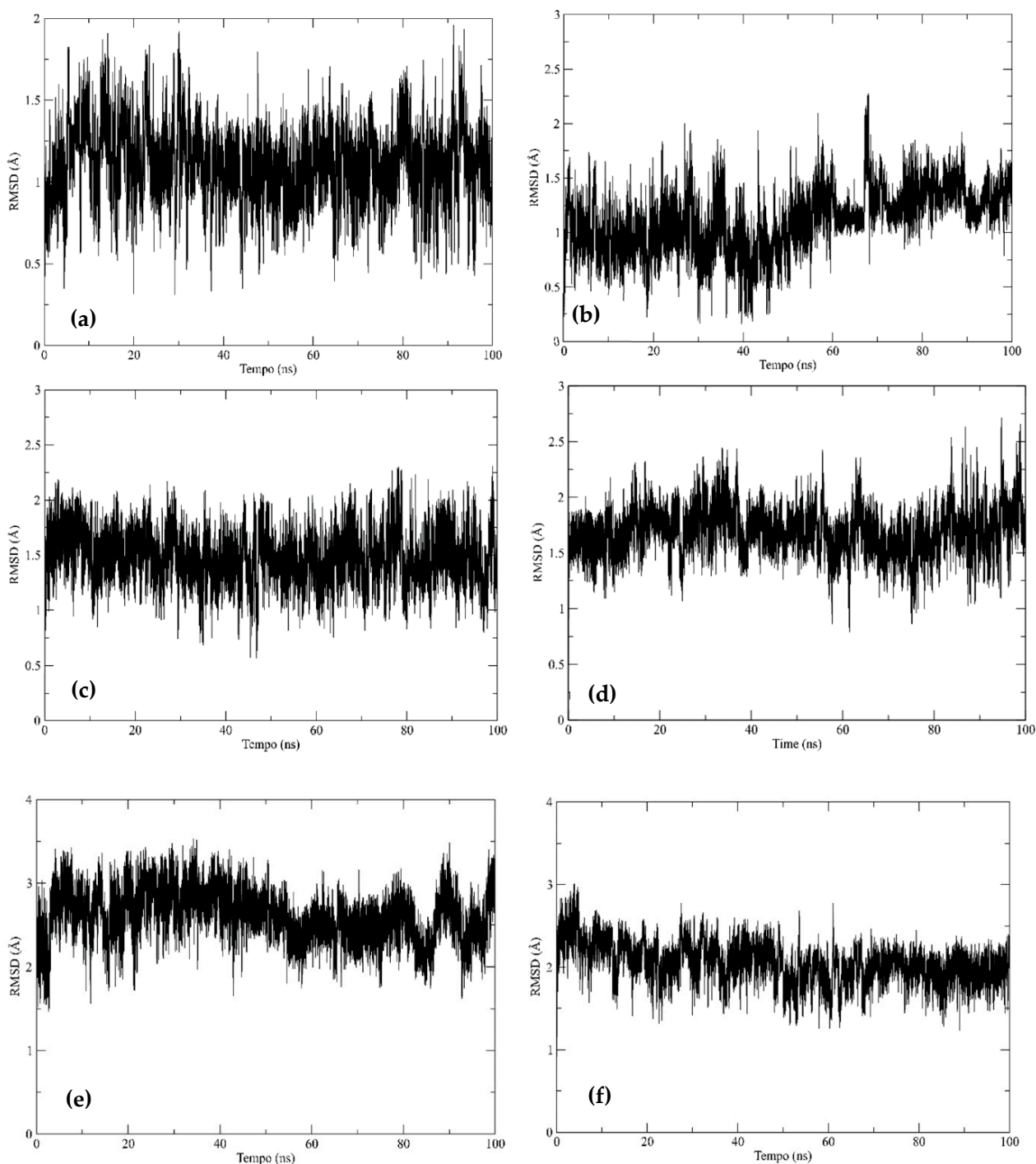
**Figure 5.** Square Root of Mean Square Deviation (*RMSD*) of the initial conformation of the complex versus the simulation time (ns) in the production stage. (**a**) Octanoic acid; (**b**) Decanoic acid; (**c**) Dodecanoic acid; (**d**) Tetradecanoic acid; (**e**) Hexadecanoic acid; (**f**) *cis*-9-octadecenoic acid.

It was observed that the *RMSD* stabilization values of the production stage ranged from 0.5 to 3.5 Å at the time analyzed. As shown in Figure 5, octanoic, decanoic, dodecanoic, and tetradecanoic acids had, on average, RMSD values below 2.0 Å. On the other hand, hexadecanoic and *cis*-9-octadecenoic presented values of around 3.0 Å. Therefore, it was concluded that there were no significant conformational changes in the complexes studied during the simulation periods [49]. Thus, the theoretical and experimental results presented in this work indicate that fatty acids from babassu oil form stable complexes with the

catalytic site of Eversa (Ser 153, His 268, and Asp 206), which may indicate a viable alternative for future applications.

It is worth noting that the data presented in this work agree with the results obtained by Qin, Zhong, and Wang (2021) [25]. These authors evaluated the affinity and molecular stability of different fatty acids (octanoic, tetradecanoic, octadecanoic, *cis*-9-octadecenoic, (9Z,12Z)-octadeca-9,12-dienoic and (9Z,12Z,15Z)-octadeca-9,12,15-trienoic acids) with T1 lipase from *Geobacillus zaliha* [25]. As in the present work, the authors observed that among the complexes studied, *cis*-9-octadecenoic acid presented one of the highest *RSMD* values and therefore one of the lowest stability values when compared to the other complexes.

Hydrogen Bonds

Another analysis refers to the number of intermolecular hydrogen bonds since these bonds are of great importance for the stability of the complex. Figure 6 shows the hydrogen bonds formed between the ligands and the lipase in the equilibration and production steps.
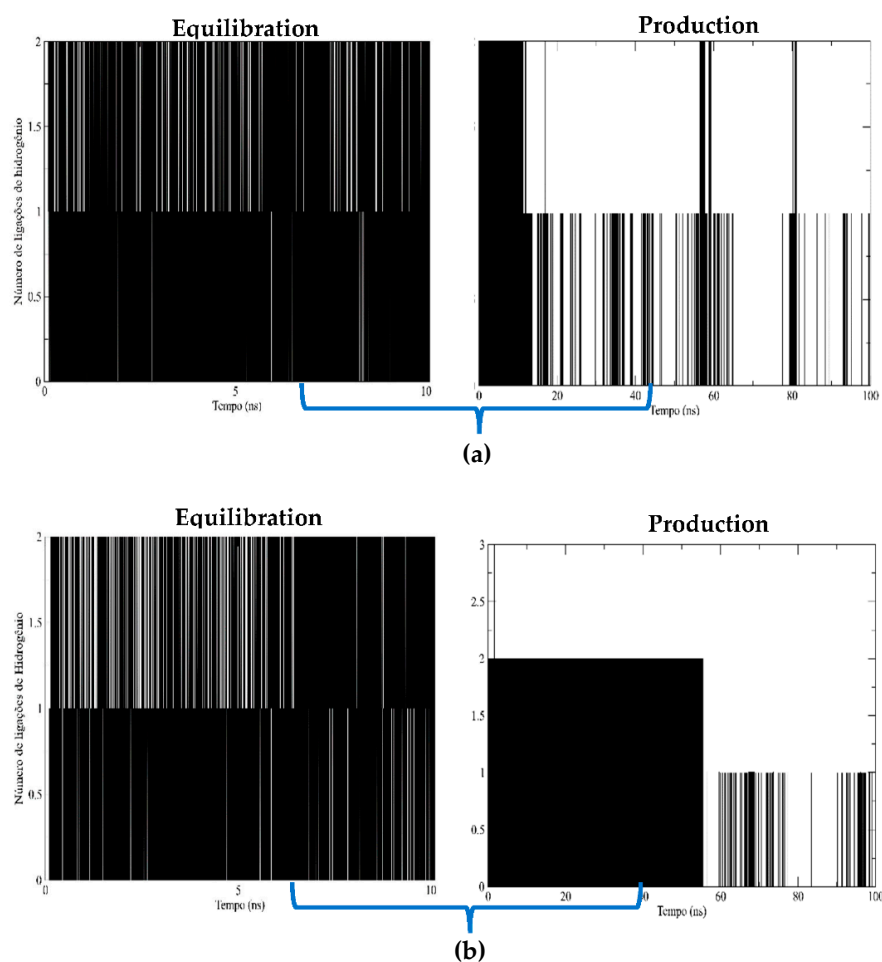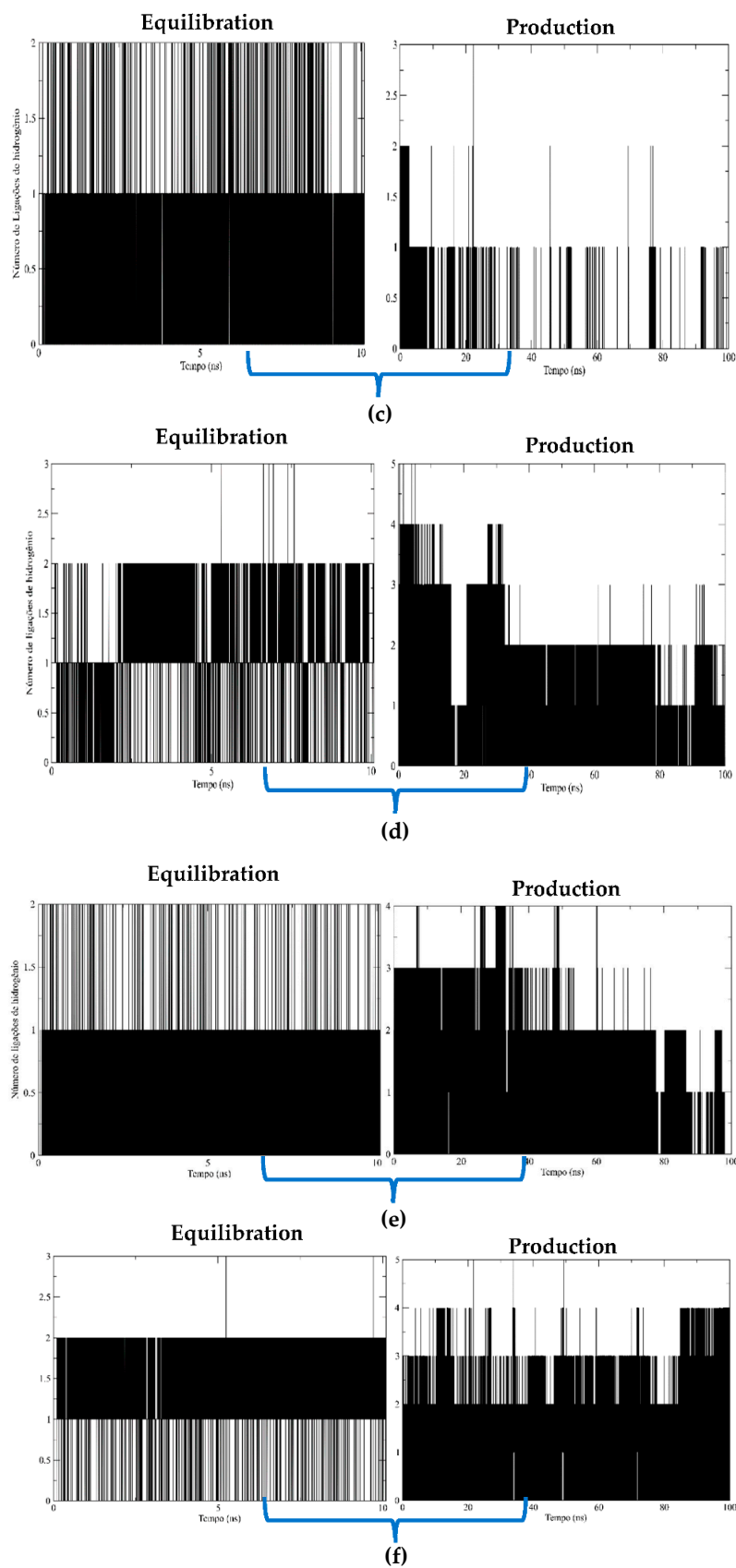


(a)



(b)

**Figure 6.** *Cont.*

**Figure 6.** Hydrogen bonds formed between the protein and the ligand during the two simulation steps. (**a**) Octanoic acid; (**b**) Decanoic acid; (**c**) Dodecanoic acid; (**d**) Tetradecanoic acid; (**e**) Hexadecanoic acid; (**f**) *cis*-9-octadecenoic acid.

The number of intermolecular hydrogen bonds is a factor of great importance for the stability of the complexes [50]. According to Figure 6, modifications occurred in the networks of hydrogen bonds throughout the simulation, so the number of bonds varied between 1 and 5. The instant in which the bonds were broken indicates that stability was maintained by the interactions of Van der Waals or hydrophobic forces [25]. Furthermore, it was possible to verify that the increase in the average number of bonds was directly related to the increase in the carbonic chain of the ligands. These results corroborate the data obtained in the molecular docking process [51]. However, it was observed that, contrary to what was exposed in the molecular docking results (Table 4), all ligands at some point formed hydrogen bonds in molecular dynamics. These results can be explained by the difference between a dynamic process (molecular dynamics) and a static process (molecular docking) [46]. In addition, the excess of exposed bonds in molecular dynamics may be due to bonds formed with the solvent of the system [25].

## 3. Materials and Methods

### 3.1. Materials

The commercial lipase Eversa® transform 2.0 from *Aspergillus oryzae* and lipase from *Thermomyces lanuginosus* were purchased from Sigma–Aldrich Brasil Ltda (Cotia, São Paulo, Brazil). All other chemical reagents used were analytical grades from Synth (São Paulo, Brazil) and Vetec (São Paulo, Brazil). Statistica® 10 software Statsoft (Tulsa, OK, USA) was used to develop the experimental design based on the Taguchi method. The refined babassu oil used in this work belongs to Leve (São Luis, Maranhão, Brazil).

### 3.2. Methods

#### 3.2.1. Hydroesterification

In this study, babassu methyl esters were obtained through the enzymatic hydroesterification process. This strategy is organized in two stages. In the first step, free fatty acids are formed using refined babassu oil via enzymatic hydrolysis using free lipase from *Thermomyces lanuginosus* (TLL) as a biocatalyst. The reaction system was developed based on the methodology proposed by Carvalho et al. (2021) [22] with adaptations. Initially, the solution containing oil and water in a 1:1 mass ratio was heated until the system reached a temperature of 40 °C. Then, 0.4% of the biocatalyst was added to the oil mass. The system remained at a temperature of 40 °C for 4 h under constant stirring.

After the process, the solution was transferred to a separatory funnel (500 mL), then 100 mL of distilled water at 60 °C was added to separate the aqueous phase from the free fatty acids (FFAs) produced. With this, the lower (aqueous) phase was excluded and the FFAs were washed three times. Then, the mixture containing the FFAs was transferred to a beaker and heated at 80 °C for 10 min. At the end of 10 min, the mixture was transferred to a funnel with filter paper and anhydrous sodium at 20% m·v$^{-1}$, which was previously dried in a muffle oven at 250 °C for 4 h [22,52].

The initial and final acid numbers (AI) (after the hydrolysis step) were calculated from Equation (1). For this, 0.3 g aliquots were removed from the reaction supernatant volume and diluted in 10 mL of ethyl alcohol. Then, 3 drops of phenolphthalein were added, followed by titration with sodium hydroxide solution [53].

$$\text{AI}\left(\frac{mgNaOH}{g}\right) = \frac{MM_{NaOH} \cdot M_{NaOH} \cdot f \cdot V_{NaOH}}{m} \tag{1}$$

where $MM_{NaOH}$ (g/mol) is the molar mass of NaOH; $M_{NaOH}$ (mol/L) is the molarity of the NaOH solution; $f$ is the correction factor determined by standardizing NaOH; $V_{NaOH}$ is the volume of NaOH used during the titration, and, $m$ (g) is the mass of the sample to be studied. The conversion of free fatty acids into esters (Equation (2)) was determined by

taking into account the initial acidity of the sample ($I_{AI}$) and of the sample after the reaction ($I_{AF}$) [52,53].

$$\text{Conversion FFA } (\%) = \left( \frac{IA_I - IA_F}{IA_I} \right) \qquad (2)$$

In the second step, direct esterification of FFAs derived from refined babassu oil and methanol was performed using lipase Eversa® Transform 2.0 in its free form as a biocatalyst. The production reactions of fatty acid methyl esters were carried out in 10 mL flasks with a lid containing the biocatalyst and the substrate on a rotary shaker with digital temperature and rotation control (TE-4200 incubator) at 200 rpm. During the studies, the temperature (25–55 °C), molar ratio between FFAs and methanol (1:1 to 1:9), percentage of biocatalyst (0.1% to 0.9%), and reaction time (1–5 h) accorded with the proposed static planning [54]. To determine the molar mass of the acids produced, the work of Figueredo et al. (2020) [55] was taken into account. The protein concentration was determined using the method described by Bradford (1976) [56], and bovine serum albumin was used as a reference.

### 3.2.2. Gas Chromatography–Mass Spectrometry (GC/MS) Analysis

For the determination of the ester content (*C*) of the obtained biodiesel samples, GC/MS analysis was performed based on the methodology described in the EN 14,103 norm [57], with adaptations. Approximately 50 mg of biodiesel sample was added to a vial (2 mL) containing 1 mL of the methyl nonadecanoate solution (10 mg/mL). This mixture was injected (1 µL) into a gas chromatograph–mass spectrometer SHIMADZU QP-2010 ULTRA (Kyoto, Japan) equipped with a (5%-phenyl)-methylpolysiloxane (DB-5) capillary column (30 m × 0.25 mm × 0.25 µm film thickness) using helium as a carrier gas in splitless mode.

### 3.2.3. Experimental Design and Statistical Analysis (Taguchi Method)

The Taguchi method used an advanced experimental design with a standard orthogonal matrix L9 (where L refers to the Latin square and 9 to the number of experiments) to determine the reaction parameters. During the study, four factors were examined at three levels to optimize the esters' production. Table 6 correlates the four independent factors (temperature, reaction time, percentage of biocatalyst, and molar ratio between FFAs and methanol) and their corresponding levels [58].

**Table 6.** Independent factors and their corresponding levels for the optimization of biodiesel production.

| Time (hours) | Temperature (°C) | Molar Ratio (FFA/Methanol) | Biocatalyst (% *w/w*) |
|---|---|---|---|
| Level 1 (L1) | 1 | 25 | 0.1 |
| Level 2 (L2) | 3 | 40 | 0.5 |
| Level 3 (L3) | 5 | 55 | 0.9 |

Statistica® software was used to elaborate the experimental design and statistical analysis. The results of the S/N ratios were obtained from the characteristics of the function "bigger is better", as this research aimed to enhance the response (conversion). The S/N ratio values were obtained from Equation (3) below [59].

$$\frac{S}{N} = -10log\left( \frac{1}{n} \sum_{i=1}^{n} 1/y_i^2 \right) \cdot 100 \qquad (3)$$

where *yi* corresponds to the response variable, *i* represents the number of repetitions, and *n* is the number of experiments for the combination of factor levels for any planning

arrangement. Through Equation (4), the expected S/N ratio was determined for the ideal conditions of the predicted maximum conversion.

$$\frac{S}{N_{PREDICTION}} = \overline{S}|R + \sum_{i=1}^{n}\left(S|R_j - \overline{S}/R\right) \tag{4}$$

where $\overline{S}|R$ refers to the arithmetic mean of all relations $S|R$, $S|R_j$ is the S/N ratio optimal for each factor, and $n$ is the number of factors significantly influencing the procedure.

### 3.2.4. Physicochemical Characterization of Babassu FAME
Kinematic Viscosity

The kinematic viscosity at 40 °C of the biodiesel produced was determined based on ASTM D-7042. An Anton Paar SVM 3000-Stabinger digital viscodensimeter (São Paulo, São Paulo, Brazil) was used during the analysis.
Density

To determine the density of oils at 20 °C, the ASTM D-7042 standard was used. For analysis, an Anton Paar SVM 3000-Stabinger digital viscodensimeter (Graz, Austria) was used.

### 3.2.5. In Silico Study
Protein Modeling by Homology

The comparative modeling of the Eversa® *Transform 2.0* lipase protein was carried out in four steps. Initially, the recognition and selection of the model protein were performed. In this step, the amino acid sequencing of the Eversa lipase protein was used, with its CAS number 9001-62-1 from the Sigma–Aldrich company. The sequence was submitted to a comparative analysis using the BLAST program (Basic Local Alignment Search Tool) www. ncbi.nih.gov/BLAST (accessed on 25 August 2022) [60] and its respective PDB database. Thus, a protein that was related to the amino acid sequence, the lipase enzyme, classified as hydrolase, was recognized by the organism *Aspergillus oryzae*, expressed through the shuttle *Escherichia coli–Pichia pastoris*, obtained from the Protein Bank (https://www.rcsb.org/) accessed on 15 March 2022, with the code 5XK2 being the target protein [61]. Then, the alignment between the sequences was performed using the Modeller program http: //www.salilab.org/modeller/ (accessed on 25 August 2022) [61]. Thus, a new protein named Eversa ® Transform 2.0 was obtained and evaluated according to the objective function and stereochemical parameters [62]. Finally, the model was approved at the stereochemical, conformational, and energetic levels. The Ramachandran graph and Verify 3D [59] determined the mold quality with the PROCHECK program https://saves.mbi. ucla.edu/ (accessed on 25 August 2022), which estimated its three-dimensional structure, indicating its three-dimensional structure and possible stereochemical quality.

Molecular Docking

A charge correction process and the addition of hydrogen atoms were carried out in the protein generated by homology—the protein generated by homology Eversa® Transform 2.0, through the Discovery Studio Visualizer Program (BIOVIA, Dassault Systémes, Discovery Studio Visualiser, San Diego, CA, USA) [63].

The structures of babassu-free fatty acids were determined using caprylic, capric, lauric, myrisitic, palmitic, and oleic acids (octanoic, decanoic, dodecanoic, tetrathnoic, hexanoic, and *cis*-9-octadecenoic acids, respectively), which together accounted for about 95% of the fatty acids present in the hydrolyzed oil. For the modulation of these structures, the software ChemDraw 3D (ChemOffice 2018, Perkin-Elmer Informatics, Shelton, CT, USA) was used, and later the structure was minimized with an MM2 force field with an RMS gradient of 0.0001.

Molecular Dynamics Simulations

For the construction of the study solutions, in addition to the molecular dynamics scripts, the CHARMM-GUI website https://www.charmm-gui.org/ (accessed on 25 August 2022) was used [64,65]. The PDB file of the complex formed by the enzyme and the ligand was chosen in its best docking pose, and a rectangular water box set at an edge distance of 10 Å from the protein was added [66]. A cubic system with an edge equal to 75 Å and crystalline angles of 90° (alpha, beta, and gamma) was then created. The periodic boundary conditions PME and FFT were generated automatically [67,68]. The force field adopted was the Charmm36m. All molecular dynamics simulations used the following fixed conditions: temperature of 313.15 K, pressure of 1 atm, and pH 7.0, and the TIP3P water model [69]. For each simulation, energy minimization was performed with ten thousand steps in ensemble NVT. Then, equilibrium simulations were performed at 10 ns in NpT ensemble. Finally, a production simulation starting at 10 ns, being extended until a situation of equilibrium of the complex was observed in the RMSD graph but never exceeding the time of 100 ns. All simulations had an integration step of 1 fs [69,70]. The graphics were visualized using Visual Molecular Dynamics (VMD) software (University of Illinois, Urbana-Champaign, IL, USA) [71].

## 4. Conclusions

This work evaluated the biocatalytic production of babassu biodiesel through enzymatic hydroesterification. This process has several advantages over conventional processes, as it allows the application of any raw material (vegetable oils, animal fats, and residual oil) regardless of its level of humidity and acidity. The proposed enzymatic hydrolysis was successfully performed since there was an increase in the acidity index of the oil from 0.75 mg NaOH/g to 127.03 mg NaOH/g.

A Taguchi design with an L9 orthogonal matrix was used to optimize the production of babassu esters. The analysis of variance of the factors related to the process (ANOVA) showed that the percentage of biocatalysts contributed significantly to the process (67.80% contribution) with a *p*-value of 0.043. Under optimal conditions (5 h of reaction at 40 °C, molar ratio FFA/alcohol 1:5, and 0.9% of biocatalyst), the theoretical conversion was 98.64%. After carrying out the proposed reaction, a 95.76% conversion was observed. The difference in the result between the theoretical conversion and the natural reaction can be explained due to the influence of external factors in the system. The kinematic viscosity and density results indicate that the biodiesel produced has potential for future applications.

The modeling of Eversa® transform 2.0 was validated by the Ramachandran graph, which showed 91.5% of the residues in favorable regions. In addition, the obtained model presented an average 3D-1D score $\geq 0.2$ of 93,71% in the Verify 3D function, proving the compatibility of the atomic model with the sequence. Thus, the modeled enzyme proved valid and suitable for further studies.

The molecular docking results suggest that the ligands studied showed an energetic affinity with the enzyme's catalytic site. It was possible to observe that all ligands studied interacted directly with the catalytic site and the oxyanion cavity. Through these results, the complexes were generated that were evaluated in molecular dynamics simulations.

Through molecular dynamics, it was possible to observe that the formed complexes accelerated high stability during the production and equivalence steps. The enzyme–substrate complexes showed low *RMSD* values, indicating that the chosen poses were appropriate for the study. The hydrogen bond graphs showed that the formed complexes showed stability, thus corroborating the data obtained in the present work. Furthermore, the theoretical and experimental results from this work indicate that fatty acids from babassu oil form stable complexes with the catalytic site of Eversa (Ser 153, His 268 and Asp 206), which may indicate a viable alternative for applications future

**Conflicts of Interest:** The authors declare no conflict of interest.

# References

1. Zhang, H.; Li, H.; Pan, H.; Liu, X.; Yang, K.; Huang, S.; Yang, S. Efficient Production of Biodiesel with Promising Fuel Properties from Koelreuteria Integrifoliola Oil Using a Magnetically Recyclable Acidic Ionic Liquid. *Energy Convers. Manag.* **2017**, *138*, 45–53. [CrossRef]

2. Abudu, H.; Sai, R. Examining Prospects and Challenges of Ghana's Petroleum Industry: A Systematic Review. *Energy Rep.* **2020**, *6*, 841–858. [CrossRef]

3. Goh, B.H.H.; Ong, H.C.; Cheah, M.Y.; Chen, W.H.; Yu, K.L.; Mahlia, T.M.I. Sustainability of Direct Biodiesel Synthesis from Microalgae Biomass: A Critical Review. *Renew. Sustain. Energy Rev.* **2019**, *107*, 59–74. [CrossRef]

4. Peng, L.; Fu, D.; Chu, H.; Wang, Z.; Qi, H. Biofuel Production from Microalgae: A Review. *Environ. Chem. Lett.* **2020**, *18*, 285–297. [CrossRef]

5. Lima, P.J.M.; da Silva, R.M.; Neto, C.A.C.G.; Gomes e Silva, N.C.; Souza, J.E.d.S.; Nunes, Y.L.; Sousa dos Santos, J.C. An Overview on the Conversion of Glycerol to Value-Added Industrial Products via Chemical and Biochemical Routes. *Biotechnol. Appl. Biochem.* **2021**. [CrossRef]

6. Temóteo, R.L.; da Silva, M.J.; de Ávila Rodrigues, F.; da Silva, W.F.; de Jesus Silva, D.; Oliveira, C.M. A Kinetic Investigation of Triacetin Methanolysis and Assessment of the Stability of a Sulfated Zirconium Oxide Catalyst. *J. Am. Oil Chem. Soc.* **2018**, *95*, 865–874. [CrossRef]

7. Staufenberg, G.; Graupner, N.; Müssig, J.; Tripathi, M.; Bhatnagar, A.; Pandey, K.K.; De, M.; Salgado, F.; Abioye, A.M.; Junoh, M.M.; et al. Preparation of Activated Carbon from Babassu Endocarpunder Microwave Radiation by Physical Activation. *IOP Conf. Series Earth Environ. Sci.* **2018**, *105*, 012116. [CrossRef]

8. Sales, M.B.; Borges, P.T.; Ribeiro Filho, M.N.; Miranda da Silva, L.R.; Castro, A.P.; Sanders Lopes, A.A.; Chaves de Lima, R.K.; de Sousa Rios, M.A.; Santos, J.C.S. dos Sustainable Feedstocks and Challenges in Biodiesel Production: An Advanced Bibliometric Analysis. *Bioengineering* **2022**, *9*, 539. [CrossRef]

9. Mota, G.F.; de Sousa, I.G.; de Oliveira, A.L.B.; Cavalcante, A.L.G.; Moreira, K.d.S.; Cavalcante, F.T.T.; Souza, J.E.D.S.; Falcão, R.d.A.; Rocha, T.G.; Valério, R.B.R.; et al. Biodiesel Production from Microalgae Using Lipase-Based Catalysts: Current Challenges and Prospects. *Algal Res.* **2022**, *62*, 102616. [CrossRef]

10. Wancura, J.H.C.; Rosset, D.v.; Mazutti, M.A.; Ugalde, G.A.; de Oliveira, J.V.; Tres, M.v.; Jahn, S.L. Improving the Soluble Lipase–Catalyzed Biodiesel Production through a Two-Step Hydroesterification Reaction System. *Appl. Microbiol. Biotechnol.* **2019**, *103*, 7805–7817. [CrossRef]

11. Cavalcante, F.T.T.; Cavalcante, A.L.G.; de Sousa, I.G.; Neto, F.S.; dos Santos, J.C.S. Current Status and Future Perspectives of Supports and Protocols for Enzyme Immobilization. *Catalysts* **2021**, *11*, 1222. [CrossRef]

12. Monteiro, R.R.C.; dos Santos, J.C.S.; Alcántara, A.R.; Fernandez-Lafuente, R. Enzyme-Coated Micro-Crystals: An Almost Forgotten but Very Simple and Elegant Immobilization Strategy. *Catalysts* **2020**, *10*, 891. [CrossRef]

13. de Oliveira, A.L.B.; Cavalcante, F.T.T.; Moreira, K.S.; Monteiro, R.R.C.; Rocha, T.G.; Souza, J.E.S.; da Fonseca, A.M.; Lopes, A.A.S.; Guimarães, A.P.; de Lima, R.K.C.; et al. Lipases Immobilized onto Nanomaterials as Biocatalysts in Biodiesel Production: Scientific Context, Challenges, and Opportunities. *Rev. Virtual Química* **2021**, *13*, 875–891. [CrossRef]

14. Marques da Fonseca, A.; Bezerra de Freitas, Í.; Baltazar Soares, N.; Aurecio Morais de Araújo, F.; Menezes Gaieta, E.; Cleiton Sousa dos Santos, J.; Carlos Nogueira Sobrinho, A.; Silva Marinho, E.; Paulo Colares, R. Synthesis, Biological Activity, and In Silico Study of Bioesters Derived from Bixin by the CALB Enzyme. *Biointerface Res. Appl. Chem.* **2021**, *12*, 5901–5917. [CrossRef]

15. Cavalcante, A.L.G.; Chaves, A.V.; Fechine, P.B.A.; Holanda Alexandre, J.Y.N.; Freire, T.M.; Davi, D.M.B.; Neto, F.S.; de Sousa, I.G.; da Silva Moreira, K.; de Oliveira, A.L.B.; et al. Chemical Modification of Clay Nanocomposites for the Improvement of the Catalytic Properties of Lipase A from Candida Antarctica. *Process Biochem.* **2022**, *120*, 1–14. [CrossRef]

16. Bonazza, H.L.; Manzo, R.M.; dos Santos, J.C.S.; Mammarella, E.J. Operational and Thermal Stability Analysis of Thermomyces Lanuginosus Lipase Covalently Immobilized onto Modified Chitosan Supports. *Appl. Biochem. Biotechnol.* **2018**, *184*, 182–196. [CrossRef] [PubMed]

17. Monteiro, R.R.C.; de Oliveira, A.L.B.; de Menezes, F.L.; de Souza, M.C.M.; Fechine, P.B.A.; dos Santos, J.C.S. Improvement of Enzymatic Activity and Stability of Lipase A from Candida Antarctica onto Halloysite Nanotubes with Taguchi Method for Optimized Immobilization. *Appl. Clay Sci.* **2022**, *228*, 106634. [CrossRef]

18. Silva, A.R.M.; Alexandre, J.Y.N.H.; Souza, J.E.S.; Neto, J.G.L.; De, S.; Júnior, P.G.; Rocha, M.V.P.; dos Santos, J.C.S.; Silva, A.R.M.; Alexandre, J.Y.N.H.; et al. The Chemistry and Applications of Metal–Organic Frameworks (MOFs) as Industrial Enzyme Immobilization Systems. *Molecules* **2022**, *27*, 4529. [CrossRef]

19. Velasco-Lozano, S.; Rocha-Martin, J.; Santos, J.C.S. dos Editorial: Designing Carrier-Free Immobilized Enzymes for Biocatalysis. *Front. Bioeng. Biotechnol.* **2022**, *10*, 823. [CrossRef]

20. Souza, J.E.D.S.; Oliveira, G.P.D.; Alexandre, J.Y.N.H.; Da, J.E.; Souza, S.; de Oliveira, G.P.; Alexandre, J.Y.N.H.; Neto, J.G.L.; Sales, M.B.; De, P.G.; et al. A Comprehensive Review on the Use of Metal–Organic Frameworks (MOFs) Coupled with Enzymes as Biosensors. *Electrochem* **2022**, *3*, 89–113. [CrossRef]

21. Garcia-Galan, C.; Barbosa, O.; Hernandez, K.; Santos, J.; Rodrigues, R.; Fernandez-Lafuente, R. Evaluation of Styrene-Divinylbenzene Beads as a Support to Immobilize Lipases. *Molecules* **2014**, *19*, 7629–7645. [CrossRef] [PubMed]

22. Carvalho, W.C.A.; Luiz, J.H.H.; Fernandez-Lafuente, R.; Hirata, D.B.; Mendes, A.A. Eco-Friendly Production of Trimethylol-propane Triesters from Refined and Used Soybean Cooking Oils Using an Immobilized Low-Cost Lipase (Eversa>® Transform 2.0) as Heterogeneous Catalyst. *Biomass Bioenergy* **2021**, *155*, 106302. [CrossRef]

23. Chang, M.Y.; Chan, E.S.; Song, C.P. Biodiesel Production Catalysed by Low-Cost Liquid Enzyme Eversa® Transform 2.0: Effect of Free Fatty Acid Content on Lipase Methanol Tolerance and Kinetic Model. *Fuel* **2021**, *283*, 119266. [CrossRef]

24. Cavalcante, F.T.T.; da Fonseca, A.M.; Holanda Alexandre, J.Y.N.; dos Santos, J.C.S. A Stepwise Docking and Molecular Dynamics Approach for Enzymatic Biolubricant Production Using Lipase Eversa® Transform as a Biocatalyst. *Ind. Crop. Prod.* **2022**, *187*, 115450. [CrossRef]

25. Qin, X.; Zhong, J.; Wang, Y. A Mutant T1 Lipase Homology Modeling, and Its Molecular Docking and Molecular Dynamics Simulation with Fatty Acids. *J. Biotechnol.* **2021**, *337*, 24–34. [CrossRef]

26. Moreira, K.d.S.; de Oliveira, A.L.B.; Júnior, L.S.d.M.; Monteiro, R.R.C.; da Rocha, T.N.; Menezes, F.L.; Fechine, L.M.U.D.; Denardin, J.C.; Michea, S.; Freire, R.M.; et al. Lipase From Rhizomucor Miehei Immobilized on Magnetic Nanoparticles: Performance in Fatty Acid Ethyl Ester (FAEE) Optimized Production by the Taguchi Method. *Front. Bioeng. Biotechnol.* **2020**, *8*, 693. [CrossRef]

27. Souza, J.E.S.; Monteiro, R.R.C.; Rocha, T.G.; Moreira, K.S.; Cavalcante, F.T.T.; de Sousa Braz, A.K.; de Souza, M.C.M.; dos Santos, J.C.S. Sonohydrolysis Using an Enzymatic Cocktail in the Preparation of Free Fatty Acid. *3 Biotech* **2020**, *10*, 1–10. [CrossRef]

28. Mohd Hussin, F.N.N.; Attan, N.; Wahab, R.A. Taguchi Design-Assisted Immobilization of Candida Rugosa Lipase onto a Ternary Alginate/Nanocellulose/Montmorillonite Composite: Physicochemical Characterization, Thermal Stability and Reusability Studies. *Enzym. Microb. Technol.* **2020**, *136*, 109506. [CrossRef]

29. Li, S.; Zhong, L.; Wang, H.; Li, J.; Cheng, H.; Ma, Q. Process Optimization of Polyphenol Oxidase Immobilization: Isotherm, Kinetic, Thermodynamic and Removal of Phenolic Compounds. *Int. J. Biol. Macromol.* **2021**, *185*, 792–803. [CrossRef]

30. Ameri, A.; Shakibaie, M.; Khoobi, M.; Faramarzi, M.A.; Ameri, A.; Forootanfar, H. Immobilization of Thermoalkalophilic Lipase from Bacillus Atrophaeus FSHM2 on Amine-Modified Graphene Oxide Nanostructures: Statistical Optimization and Its Application for Pentyl Valerate Synthesis. *Appl. Biochem. Biotechnol.* **2020**, *191*, 579–604. [CrossRef]

31. Babaki, M.; Yousefi, M.; Habibi, Z.; Mohammadi, M. Process Optimization for Biodiesel Production from Waste Cooking Oil Using Multi-Enzyme Systems through Response Surface Methodology. *Renew. Energy* **2017**, *105*, 465–472. [CrossRef]

32. Arana-Peña, S.; Carballares, D.; Morellon-Sterlling, R.; Berenguer-Murcia, Á.; Alcántara, A.R.; Rodrigues, R.C.; Fernandez-Lafuente, R. Enzyme Co-Immobilization: Always the Biocatalyst Designers' Choice . . . or Not? *Biotechnol. Adv.* **2021**, *51*, 107584. [CrossRef] [PubMed]

33. Monteiro, R.R.C.; Arana-Peña, S.; da Rocha, T.N.; Miranda, L.P.; Berenguer-Murcia, Á.; Tardioli, P.W.; dos Santos, J.C.S.; Fernandez-Lafuente, R. Liquid Lipase Preparations Designed for Industrial Production of Biodiesel. Is It Really an Optimal Solution? *Renew. Energy* **2021**, *164*, 1566–1587. [CrossRef]

34. Sun, S.; Guo, J.; Chen, X. Biodiesel Preparation from Semen Abutili (Abutilon Theophrasti Medic.) Seed Oil Using Low-Cost Liquid Lipase Eversa® Transform 2.0 as a Catalyst. *Ind. Crop. Prod.* **2021**, *169*, 113643. [CrossRef]

35. Adewale, P.; Vithanage, L.N.; Christopher, L. Optimization of Enzyme-Catalyzed Biodiesel Production from Crude Tall Oil Using Taguchi Method. *Energy Convers. Manag.* **2017**, *154*, 81–91. [CrossRef]

36. Knothe, G.; Steidley, K.R. Kinematic Viscosity of Biodiesel Fuel Components and Related Compounds. Influence of Compound Structure and Comparison to Petrodiesel Fuel Components. *Fuel* **2005**, *84*, 1059–1065. [CrossRef]

37. Ramírez Verduzco, L.F. Density and Viscosity of Biodiesel as a Function of Temperature: Empirical Models. *Renew. Sustain. Energy Rev.* **2013**, *19*, 652–665. [CrossRef]

38. Tam, B.; Sinha, S.; Wang, S.M. Combining Ramachandran Plot and Molecular Dynamics Simulation for Structural-Based Variant Classification: Using TP53 Variants as Model. *Comput. Struct. Biotechnol. J.* **2020**, *18*, 4033–4039. [CrossRef]

39. Sarkar, S.; Banerjee, A.; Chakraborty, N.; Soren, K.; Chakraborty, P.; Bandopadhyay, R. Structural-Functional Analyses of Textile Dye Degrading Azoreductase, Laccase and Peroxidase: A Comparative in Silico Study. *Electron. J. Biotechnol.* **2020**, *43*, 48–54. [CrossRef]

40. Bronowska, A.K. Thermodynamics of Ligand-Protein Interactions: Implications for Molecular Design. *Thermodyn. Interact. Stud. Solids Liq. Gases* **2011**. [CrossRef]

41. Lan, D.; Zhao, G.; Holzmann, N.; Yuan, S.; Wang, J.; Wang, Y. Structure-Guided Rational Design of a Mono- And Diacylglycerol Lipase from Aspergillus Oryzae: A Single Residue Mutant Increases the Hydrolysis Ability. *J. Agric. Food Chem.* **2021**, *69*, 5344–5352. [CrossRef]

42. Zhang, M.; Li, Q.; Lan, X.; Li, X.; Zhang, Y.; Wang, Z.; Zheng, J. Directed Evolution of Aspergillus Oryzae Lipase for the Efficient Resolution of (R,S)-Ethyl-2-(4-Hydroxyphenoxy) Propanoate. *Bioprocess Biosyst. Eng.* **2020**, *43*, 2131–2141. [CrossRef] [PubMed]

43. He, Y.; Li, J.; Kodali, S.; Balle, T.; Chen, B.; Guo, Z. Liquid Lipases for Enzymatic Concentration of N-3 Polyunsaturated Fatty Acids in Monoacylglycerols via Ethanolysis: Catalytic Specificity and Parameterization. *Bioresour Technol* **2017**, *224*, 445–456. [CrossRef] [PubMed]

44. Tamboli, A.S.; Waghmare, P.R.; Khandare, R.v.; Govindwar, S.P. Comparative Analyses of Enzymatic Activity, Structural Study and Docking of Fungal Cellulases. *Gene Rep.* **2017**, *9*, 54–60. [CrossRef]

45. Liu, Z.; Liu, Y.; Zeng, G.; Shao, B.; Chen, M.; Li, Z.; Jiang, Y.; Liu, Y.; Zhang, Y.; Zhong, H. Application of Molecular Docking for the Degradation of Organic Pollutants in the Environmental Remediation: A Review. *Chemosphere* **2018**, *203*, 139–150. [CrossRef]

46. Fatma, T.; Zafar, Z.; Fatima, S.; Paracha, R.Z.; Adnan, F.; Sheikh, Z.; Virk, N.; Bhatti, M.F. Computational Assessment of Botrytis Cinerea Lipase for Biofuel Production. *Catalysts* **2021**, *11*, 1319. [CrossRef]

47. Williams, D.H.; Westwell, M.S. Aspects of Weak Interactions. *Chem. Soc. Rev.* **1998**, *27*, 57–64. [CrossRef]

48. Guimarães, J.R.; Miranda, L.P.; Fernandez-Lafuente, R.; Tardioli, P.W. Immobilization of Eversa® Transform via CLEA Technology Converts It in a Suitable Biocatalyst for Biolubricant Production Using Waste Cooking Oil. *Molecules* **2021**, *26*, 193. [CrossRef]

49. Joshi, T.; Joshi, T.; Sharma, P.; Chandra, S.; Pande, V. Molecular Docking and Molecular Dynamics Simulation Approach to Screen Natural Compounds for Inhibition of Xanthomonas Oryzae Pv. Oryzae by Targeting Peptide Deformylase. *J. Biomol. Struct. Dyn.* **2020**, *39*, 823–840. [CrossRef]

50. Ragunathan, A.; Malathi, K.; Anbarasu, A. MurB as a Target in an Alternative Approach to Tackle the Vibrio Cholerae Resistance Using Molecular Docking and Simulation Study. *J. Cell. Biochem.* **2018**, *119*, 1726–1732. [CrossRef]

51. Qu, P.; Li, D.; Lazim, R.; Xu, R.; Xiao, D.; Wang, F.; Li, X.; Zhang, Y. Improved Thermostability of Thermomyces Lanuginosus Lipase by Molecular Dynamics Simulation and in Silico Mutation Prediction and Its Application in Biodiesel Production. *Fuel* **2022**, *327*, 125039. [CrossRef]

52. Moreira, K.S.; Moura, L.S.; Monteiro, R.R.C.; de Oliveira, A.L.B.; Valle, C.P.; Freire, T.M.; Fechine, P.B.A.; de Souza, M.C.M.; Fernandez-Lorente, G.; Guisan, J.M.; et al. Optimization of the Production of Enzymatic Biodiesel from Residual Babassu Oil (Orbignya Sp.) via RSM. *Catalysts* **2020**, *10*, 414. [CrossRef]

53. Monteiro, R.R.C.; Neto, D.M.A.; Fechine, P.B.A.; Lopes, A.A.S.; Gonçalves, L.R.B.; dos Santos, J.C.S.; de Souza, M.C.M.; Fernandez-Lafuente, R. Ethyl Butyrate Synthesis Catalyzed by Lipases A and B from Candida Antarctica Immobilized onto Magnetic Nanoparticles. Improvement of Biocatalysts' Performance under Ultrasonic Irradiation. *Int. J. Mol. Sci.* **2019**, *20*, 5807. [CrossRef] [PubMed]

54. Rocha, T.G.; de L. Gomes, P.H.; de Souza, M.C.M.; Monteiro, R.R.C.; dos Santos, J.C.S. Lipase Cocktail for Optimized Biodiesel Production of Free Fatty Acids from Residual Chicken Oil. *Catal Lett.* **2021**, *151*, 1155–1166. [CrossRef]

55. Figueredo, I.D.M.; Rios, M.A.D.S.; Cavalcante, C.L.; Luna, F.M.T. Effects of Amine and Phenolic Based Antioxidants on the Stability of Babassu Biodiesel Using Rancimat and Differential Scanning Calorimetry Techniques. *Ind. Eng. Chem. Res.* **2020**, *59*, 18–24. [CrossRef]

56. Bradford, M.M. A Rapid and Sensitive Method for the Quantitation of Microgram Quantities of Protein Utilizing the Principle of Protein-Dye Binding. *Anal. Biochem.* **1976**, *72*, 248–254. [CrossRef]

57. *BSI BS EN 14103*; Fat and Oil Derivatives-Fatty Acid Methyl Esters (FAME)-Determination of Ester and Linolenic Acid Methyl Ester Contents. European Committee for Standardization, Management Centre: Bruxelles, Belgium, 2011; Volume 17, pp. 1–22.

58. Moreira, K.D.S.; de Oliveira, A.L.B.; Júnior, L.S.D.M.; de Sousa, I.G.; Cavalcante, A.L.G.; Neto, F.S.; Valério, R.B.R.; Chaves, A.V.; Fonseca, T.D.S.; Cruz, D.M.V.; et al. Taguchi Design-Assisted Co-Immobilization of Lipase A and B from Candida Antarctica onto Chitosan: Characterization, Kinetic Resolution Application, and Docking Studies. *Chem. Eng. Res. Des.* **2022**, *177*, 223–244. [CrossRef]

59. Chakraborty, R.; RoyChowdhury, D. Fish Bone Derived Natural Hydroxyapatite-Supported Copper Acid Catalyst: Taguchi Optimization of Semibatch Oleic Acid Esterification. *Chem. Eng. J.* **2013**, *215–216*, 491–499. [CrossRef]

60. Altschul, S.F.; Gish, W.; Miller, W.; Myers, E.W.; Lipman, D.J. Basic Local Alignment Search Tool. *J. Mol. Biol.* **1990**, *215*, 403–410. [CrossRef]

61. Webb, B.; Sali, A. Comparative Protein Structure Modeling Using MODELLER. *Curr. Protoc. Bioinform.* **2016**, *54*, 5.6.1–5.6.37. [CrossRef]

62. Bedoya, O.F.; Tischer, I. Detección de Homología Remota de Proteínas Usando Modelos 3D Enriquecidos Con Propiedades Fisicoquímicas. *Ing. Y Compet.* **2015**, *17*, 75–84. [CrossRef]

63. Morris, G.M.; Ruth, H.; Lindstrom, W.; Sanner, M.F.; Belew, R.K.; Goodsell, D.S.; Olson, A.J. AutoDock4 and AutoDockTools4: Automated Docking with Selective Receptor Flexibility. *J. Comput. Chem.* **2009**, *30*, 2785–2791. [CrossRef] [PubMed]

64. Lee, J.; Cheng, X.; Swails, J.M.; Yeom, M.S.; Eastman, P.K.; Lemkul, J.A.; Wei, S.; Buckner, J.; Jeong, J.C.; Qi, Y.; et al. CHARMM-GUI Input Generator for NAMD, GROMACS, AMBER, OpenMM, and CHARMM/OpenMM Simulations Using the CHARMM36 Additive Force Field. *J. Chem. Theory Comput.* **2016**, *12*, 405–413. [CrossRef] [PubMed]

65. Brooks, B.R.; Brooks, C.L.; Mackerell, A.D.; Nilsson, L.; Petrella, R.J.; Roux, B.; Won, Y.; Archontis, G.; Bartels, C.; Boresch, S.; et al. CHARMM: The Biomolecular Simulation Program. *J. Comput. Chem.* **2009**, *30*, 1545–1614. [CrossRef] [PubMed]

66. Jorgensen, W.L.; Chandrasekhar, J.; Madura, J.D.; Impey, R.W.; Klein, M.L. Comparison of Simple Potential Functions for Simulating Liquid Water. *J. Chem. Phys.* **1983**, *79*, 926–935. [CrossRef]

67. Cheatham, T.E.; Miller, J.L.; Fox, T.; Darden, T.A.; Kollman, P.A. Molecular Dynamics Simulations on Solvated Biomolecular Systems: The Particle Mesh Ewald Method Leads to Stable Trajectories of DNA, RNA, and Proteins. *J. Am. Chem. Soc.* **1995**, *117*, 4193–4194. [CrossRef]

68. Hess, B.; Bekker, H.; Berendsen, H.J.C.; Fraaije, J.G.E.M. LINCS: A Linear Constraint Solver for Molecular Simulations. *J. Comput. Chem.* **1997**, *18*, 1463–1472. [CrossRef]

69. Phillips, J.C.; Hardy, D.J.; Maia, J.D.C.; Stone, J.E.; Ribeiro, J.v.; Bernardi, R.C.; Buch, R.; Fiorin, G.; Hénin, J.; Jiang, W.; et al. Scalable Molecular Dynamics on CPU and GPU Architectures with NAMD. *J. Chem. Phys.* **2020**, *153*, 044130. [CrossRef]

70. Field, M.J.; Albe, M.; Bret, C.; Proust-De Martin, F.; Thomas, A. The Dynamo Library for Molecular Simulations Using Hybrid Quantum Mechanical and Molecular Mechanical Potentials. *J. Comput. Chem.* **2000**, *21*, 1088–1100. [CrossRef]

71. Humphrey, W.; Dalke, A.; Schulten, K. VMD: Visual Molecular Dynamics. *J. Mol. Graph.* **1996**, *14*, 33–38. [CrossRef]